

On the Accuracy of Hypocenter Determination of the Hokuriku Microearthquake Observatory

Kunihiko WATANABE, Norio HIRANO and Fumiaki TAKEUCHI

(Manuscript received December 27, 1978)

Abstract

The accuracy of a method of hypocenter determination which was carried out as a routine work at the Hokuriku Microearthquake Observatory was investigated. A telemetering observation system with seven satellite stations was completed in 1976 at the Observatory, with a time accuracy of 20 milliseconds.

In this article, the accuracy of hypocenter determination is discussed principally from the viewpoint of errors of reading seismograms and the propriety of analysis methods.

The accuracy of reading seismograms was examined by comparing the results read independently by two persons on a pen-recording seismogram with a paper-speed of 8 mm/sec. The results show that the reading errors caused by the reader's personality are estimated as, at most, 0.1 s for P-wave and 0.5 s for origin time converted from S-P time.

Variations of hypocenters were calculated by giving observational errors Δt in various ways, in which Δt is 0.1 s for P arrival times or 0.5 s for the origin times. The results are as follows: Variations of epicenters are less than 2 km in the neighbourhood of the network, and are about 5 km apart from it. In the middle distant area, the operation of adding Δt mainly affects the depths of hypocenters.

The variation of hypocenters caused by the differences of combinations of stations and of the sampling of the assumed P-wave velocity data were also examined. These results show that the variations are small enough to discuss seismic activity.

From these results, it seems important for the accurate determination of hypocenters to know crustal structure as correctly as possible.

1. Introduction

At the Hokuriku Microearthquake Observatory, Disaster Prevention Research Institute, Kyoto University, determinations of hypocenter and magnitude have been carried out as its routine work, because detecting any anomalous seismic activity and responding to it without delay are necessary for the investigation of earthquake prediction.

It is, however, rather a difficult task to determine the exact locations of hypocenters and also to estimate their errors^{1), 2)}. The accuracy of hypocenter determination is affected by many factors, such as 1) accuracy of observation, 2) propriety of the crustal model, 3) reading errors of seismograms, 4) precision of analysis method, and others. As a telemetering system was introduced in 1976 at this Observatory, the time accuracy of observation was raised to very high value of about 20 milliseconds. Details about the telemetering system are found in Kishimoto et al (1978)³⁾. As for 2), although some investigations of the crustal structure are in progress by

use of several explosions and natural earthquakes, a tentative structure as shown in Fig. 5 was assumed here, referring to the results of seismic explorations of Atsumi-Noto⁴⁾, Miboro⁵⁾ and Hanabusa-Kurayoshi⁶⁾.

In this article, therefore, we shall treat principally with problems 3) and 4), namely estimate of errors in reading seismograms and accuracy of the analysis method used.

2. Microseismic data and those accuracy

Discussions on the telemetering system at the Observatory have already been done by Kishimoto et al (1978). A trigger consisting of some AND and OR circuits is included in this system, which contains some kinds of judgements, namely, judgements about amplitude, frequency and time interval of seismic signal continuation. Following the trigger signals, seismic data are recorded by a magnetic tape recorder and a visible recorder (14 chs, 8 mm/sec). The timing accuracy of seismic data is, in the case of sharply rising initial motion, better than 30 milliseconds.

Earthquakes with more than three P -readings and one or more $S-P$ readings are adopted. If any $S-P$ time is clearly so long as to indicate distant earthquakes, the record is left unread. Concerning the visible record (14 chs, 8 mm/sec), reading of seismograms is carried out by an $X-Y$ digitizer. Calculation is done by a mini-computer equipped at the Observatory, because it is important to catch seismic activity on the spot.

The number of earthquakes, P -times and $S-P$ times vary with the person who reads the records, for each reader has his own basis of reading. When we discuss the accuracy of seismic data, it is important to grasp the extent of this variation.

Table 1. Comparison of number of earthquakes of which three or more P -times are read. P_T and P_H denote the number of P -times read by two of the authors, Takeuchi and Hirano, respectively.

$P_T \backslash P_H$	0	1	2	3	4	5	6	7	total
0	0	0	0	2	2	3	0	3	10
1	0	0	0	0	0	0	0	0	0
2	0	0	0	0	0	0	0	0	0
3	3	0	0	9	8	3	0	0	23
4	2	0	0	2	14	15	10	8	51
5	0	0	0	0	3	19	7	9	38
6	2	0	0	0	0	1	3	8	14
7	0	0	0	0	0	0	1	9	10
total	7	0	0	13	27	41	21	37	146

In order to check this problem, the records of April '78, containing 146 earthquakes, were read by two of the authors, Takeuchi and Hirano, and individual variations were examined.

As is shown in Table 1, the number of earthquakes of which three or more P -times were read by both readers was 129 out of 146 events. The number of earthquakes read by Hirano but not by Takeuchi was 7 and the opposite one 10. Nine of these events were distant, 4 were erroneous and 1 was deep. The remaining 3 were events which successively occurred and the first arrivals were not clear. One of the successive events was a quarry blast and others were the aftershocks of an event ($M=4.7$) near Eiheiiji Temple, Fukui Prefecture, on April 3rd, 1978.

Four records with a lot of errors were examined again by the two readers, and only one was saved to use. Therefore, the number of the earthquakes which whether it is read and picked up or not depends on the reader's eyes was only one.

P -time readings by the two readers were compared. There were 579 P -times which were read by the two readers out of 129 earthquakes mentioned above. Fig. 1 shows the frequency distribution of $P_T - P_H$, where P_T and P_H are the P -times read by Takeuchi and Hirano, respectively, and suffixed T and H will be used samely hereafter.

It may be seen that only 17 sets of P_T and P_H are very different from each other, namely $|P_T - P_H|$ is greater than 0.2 s. (Fig. 1). More than 90% of the sets are within a difference of 0.1 s. Especially, the P -times, whose difference is less than 0.01 s, are marked in number. The result is shown in Fig. 1. As for the Figure, it was caused by the reader's own basis of reading that the pattern of frequency distribution was inclined towards the negative side.

Lastly, the result of S -phase is shown in Fig. 2. We treated 289 S -times. The pattern of frequency distribution is also assymmetric, because of the same reason as described above.

We used $S - P$ times to calculate origin times by a equation $P - 1.366 \times (S - P)$. Fig. 3 shows the frequency distribution of $O_T - O_H$, difference of origin times. Inclination to the positive side is reasonable judging from the process of derivation. More than 90% of origin times were within a difference of 0.5 s, and the most frequent case was that the two times coincided within a 0.05 s difference. The averaged value of the differences was about +0.05 s and this was the systematic difference of origin times caused by the difference of the reader's judgement.

3. Method of hypocenter determination

At first, a travel time table is calculated based upon the model structure of P -wave velocity, and is used to determine hypocenters. Calculation of a hypocenter is carried out as follows.

Let the three dimensional co-ordinates of i 'th station be $(X_i, Y_i, 0)$, and the P -wave arrival time at this station be P_i . T_0 should be the origin time of an event. If we assume the depth of the hypocenter is H_j , then we get

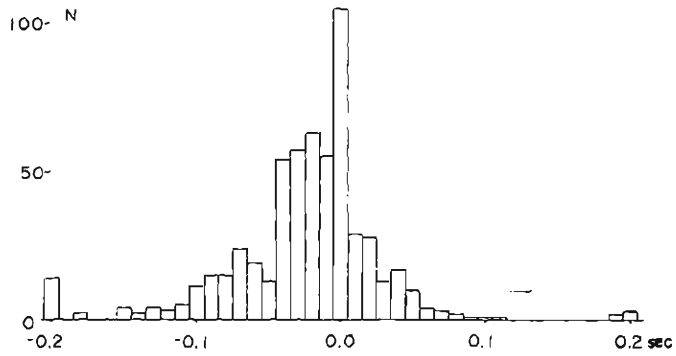


Fig. 1. Frequency distribution of $P_T - P_H$, where P_T and P_H are the P -times read by two of the authors respectively.

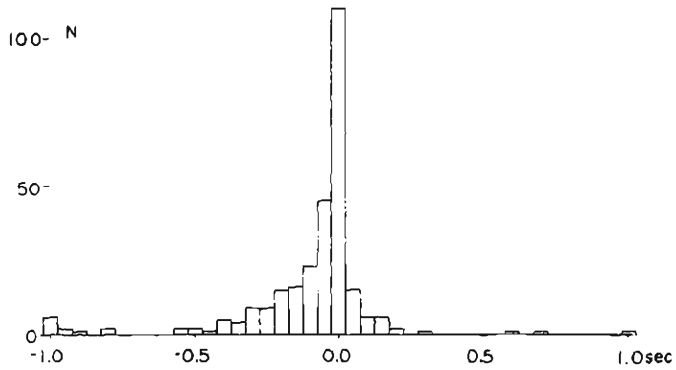


Fig. 2. Frequency distribution of $S_T - S_H$, where S_T and S_H are the S -times read by two of the authors respectively.

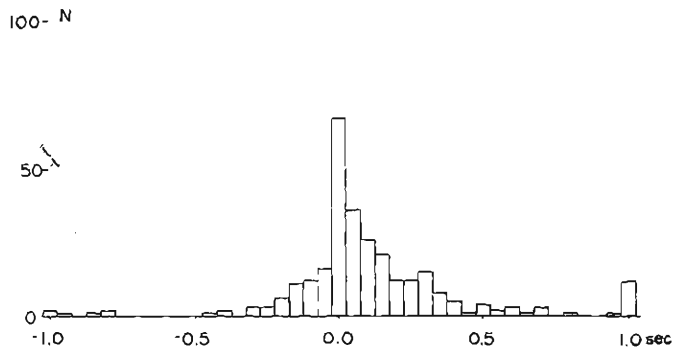


Fig. 3. Frequency distribution of $O_T - O_H$, where O_T and O_H are the origin times calculated from the data read by two of the authors respectively.

$$(XO_j - X_i)^2 + (YO_j - Y_i)^2 = R_{i,j}^2 \quad (1)$$

$$(i=1, 2, \dots, n; n \geq 3)$$

where $R_{i,j} = f(P_i - T_0, H_j)$, and

XO_j, YO_j are the two co-ordinates of the hypocenter of depth H_j .

The term $f(P_i - T_0, H_j)$ can be calculated referring to the travel time table, if the travel time $P_i - T_0$ and the depth of the hypocenter H_j are given. T_0 is fixed by the use of $S-P$ times, which may be mentioned in the later section. Equation (1) leads to

$$2XO_j(X_i - X_{i+1}) + 2YO_j(Y_i - Y_{i+1}) = X_i^2 + Y_i^2 - X_{i+1}^2 - Y_{i+1}^2 - R_{i,j}^2 + R_{i+1,j}^2 \quad (2)$$

$$(i=1, 2, \dots, n-1; n \geq 3)$$

Then XO_j and YO_j are solved by the least square method as,

$$XO_j = (\sum A_i C_i \cdot \sum B_i^2 - \sum A_i B_i \cdot \sum B_i C_i) / D$$

$$YO_j = (\sum A_i^2 \cdot \sum B_i C_i - \sum A_i C_i \cdot \sum A_i B_i) / D$$

where, $D = \sum A_i^2 \cdot \sum B_i^2 - (\sum A_i B_i)^2$

$$A_i = 2(X_i - X_{i+1})$$

$$B_i = 2(Y_i - Y_{i+1})$$

$$C_i = X_i^2 + Y_i^2 - X_{i+1}^2 - Y_{i+1}^2 - R_{i,j}^2 + R_{i+1,j}^2$$

and we deal with them only when $D \neq 0$.

We also calculate α_j by the next equations and use the value as an indicator of hypocenter determination accuracy.

$$\alpha_j = \left(\frac{1}{n} \sum (R_{i,j} - r_{i,j})^2 \right)^{1/2} \quad (3)$$

where $r_{i,j} = ((XO_j - X_i)^2 + (YO_j - Y_i)^2)^{1/2}$

Sets of these four values ($XO_j, YO_j, H_j, \alpha_j; j=1,2,\dots, m$) can be obtained according to the assumed depth H_j . “ j ” which gives the minimum of $\alpha_j (j=1,2,\dots, m)$ will be re-written as “ k ”, and then the set of hypocenter co-ordinates we are looking for is (XO_k, YO_k, H_k). This method is similar to that of figuredrawing by a pair of compasses, and is easy to program for mini-computers.

4. On the simulation for checking precision of analysis

4.1 Fictitious hypocenters

We selected 35 points in the $X-Y$ plane as the fictitious epicenters. These points satisfy the following conditions. They are, as a rule, on the mesh points of 50 km distance starting from the origin (36°N, 136°E). But some points were slightly moved and a few points were added to simulate better the microearthquake activity in the region. Every point has its neighbouring point within a circle of a radius of 60 km. The depths of the points are so selected that at least one value should be distributed in any of the layers. Then we decided to use 2, 6, 10, 26 and 38 km

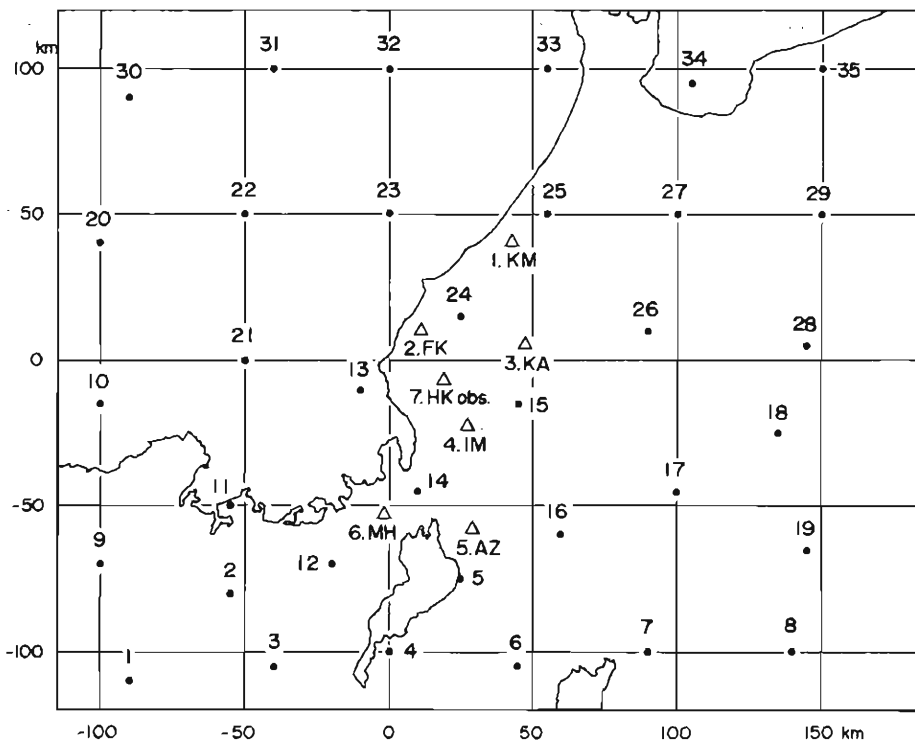


Fig. 4. Locations of fictitious epicenters and observation stations.

as depths, because the routine analysis at the Observatory concerns earthquakes occurring only from 0 to 40 km in depth. In this choice, we also considered the earthquake concentration depths in our field. Fig. 4 shows the 35 fictitious points with observation stations.

4.2 Model of P-wave velocity structure

Model of P-wave velocity structure is shown in Fig. 5. This model is assembled by considering the results of seismic explorations of Atsumi-Noto, Miboro and Hanabusa-Kurayoshi. S-wave velocities are not necessary in our case but only Poisson's ratio σ , being assumed as 0.25 all over the region, is needed to calculate an origin time. A travel time table was prepared based on the model for 21 depths of every 2 km between 0 to 40 km. We selected 11 epicentral distances between 0 to 200 km and applied linear interpolation for distances between two neighbouring points. Let us call this time table the 11-21 model. Travel times from the fictitious hypocenters to the observation stations were calculated depending on the 11-21 model.

4.3 Examination of hypocenter determination program

To examine the accuracy of the program, model travel times from the fictitious

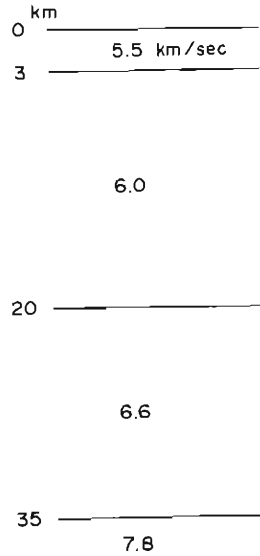


Fig. 5. P-wave velocity structure model used in hypocenter calculation.

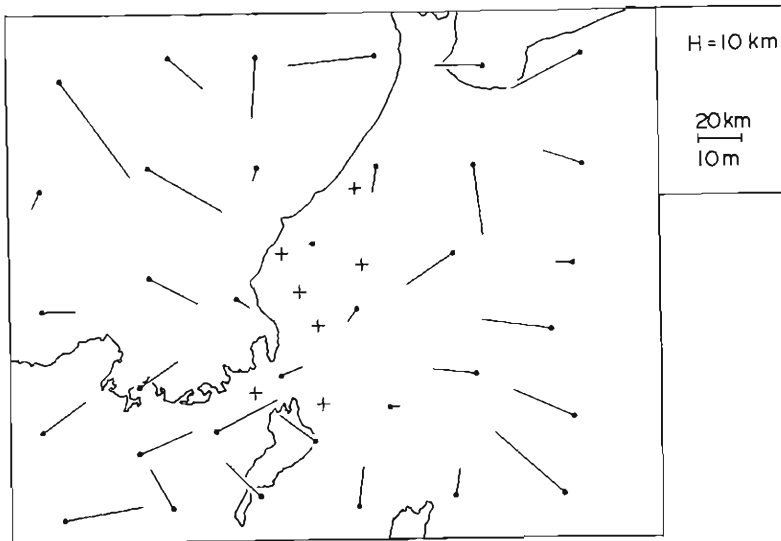


Fig. 6. Differences between the fictitious hypocenters and calculated ones. The depth is equal to 10 km.

hypocenter to the seven stations, which can be calculated by the use of the 11-21 model, are used and the hypocenter co-ordinates are again calculated. If the program is correct, the calculated hypocenter should be at the same point as the initial location. Differences of calculated hypocenters from the fictitious ones are plotted in Fig. 6 for the depth equal to 10 km, for example. The differences are small (~ 0.015 km)

when the epicenters are near the network, and they remain small even for the farther earthquakes (0.01~0.03 km). Directions of the differences are not systematic. (Fig. 6). Same arguments can be held for other depths. Irregularity of the differences may arise from the fact that the travel times are calculated based on a layered model. The differences, however, are less than 1/10 of those associated with reading errors (to be mentioned later), so this program seems to be accurate enough to calculate hypocenter locations.

4.4 Adding Δt to P-times

As mentioned above, more than 90% of P-times were read within a difference of 0.1 s by the two readers. So simulation can be achieved by giving 0.1 s as Δt to P-times.

4.4.1 Adding $|\Delta t| = 0.1$ s to one P-time

In this section, hypocenters are calculated when 0.1 s is added to any one of the P-times. Then the $S-P$ time of this station becomes shorter by 0.1 s, and so the origin time of this earthquake comes later by 0.034 s. Because, as an origin time, we adopted the average value of 7 provisional origin times calculated for each station respectively by the said equation, $P-1.366 \times (S-P)$.

Differences between the relocated epicenters and the initial ones are shown in

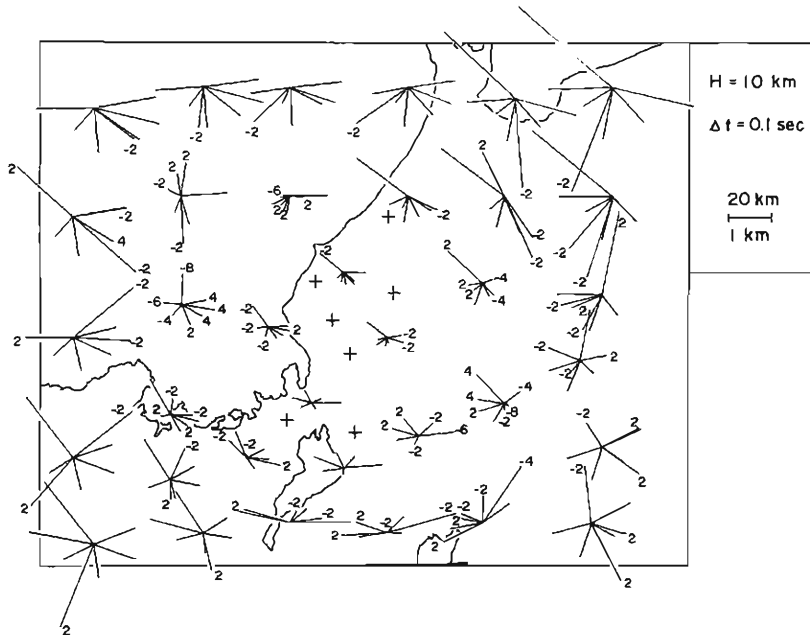


Fig. 7. Differences between the fictitious hypocenters and the relocated ones calculated from the data which 0.1 s is added to one of P-times. The relocated hypocenter subtracted by initial one is each numeral at the tip of the line denoted in km.

Fig. 7 for 10 km depth. The differences are small near the center of the network, whereas at the regions apart from the center, Δt affects the vertical co-ordinates markedly. This is explained by the fact that the travel time curves are close to each other at the epicentral distance of about 80 km. Farther than this distance, the differences are large in the horizontal plane, which is reasonable because the travel time curves are not so crowded and the differential coefficient $d\Delta/dT$ becomes larger. The directions of differences seem to turn to the center of the network as a whole. This is due to the fact that the travel times become shorter as the origin time is substituted by the later one. These results are arranged in Table 2.

Differences of epicenters were not larger than 1 km for about 70% of the cases,

Table 2. Differences between the fictitious hypocenters and the relocated ones with depth, when the deviation value, Δt , is added to one of the P -times.

Err. dep.	$\Delta \leq 1.0$ km	$\Delta \leq 2.0$ km	$ \text{dep} \leq 2$ km
2 km	70.2%	97.1%	91.0%
6	78.4	98.4	90.2
10	77.1	98.0	93.9
26	74.3	98.4	97.6
38	57.1	79.6	73.5

total=245

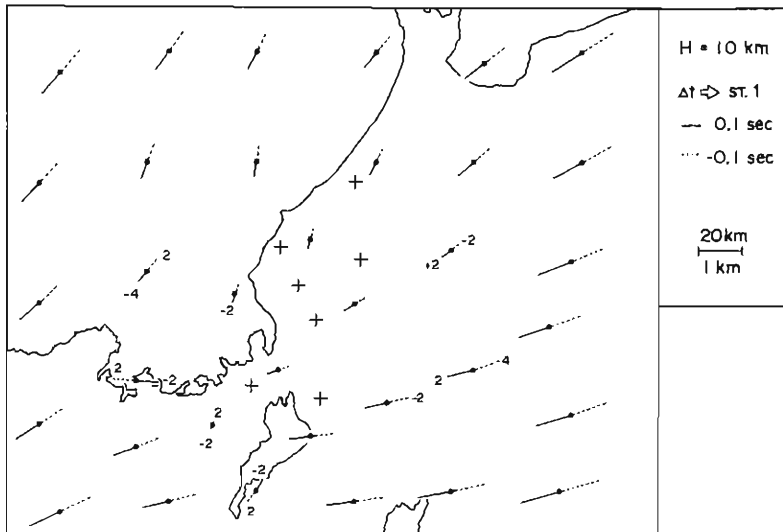


Fig. 8. Differences between the fictitious hypocenters and the relocated ones calculated from the data which ± 0.1 s have been added to the P -time of station 1. Each numeral is the same as in Fig. 7.

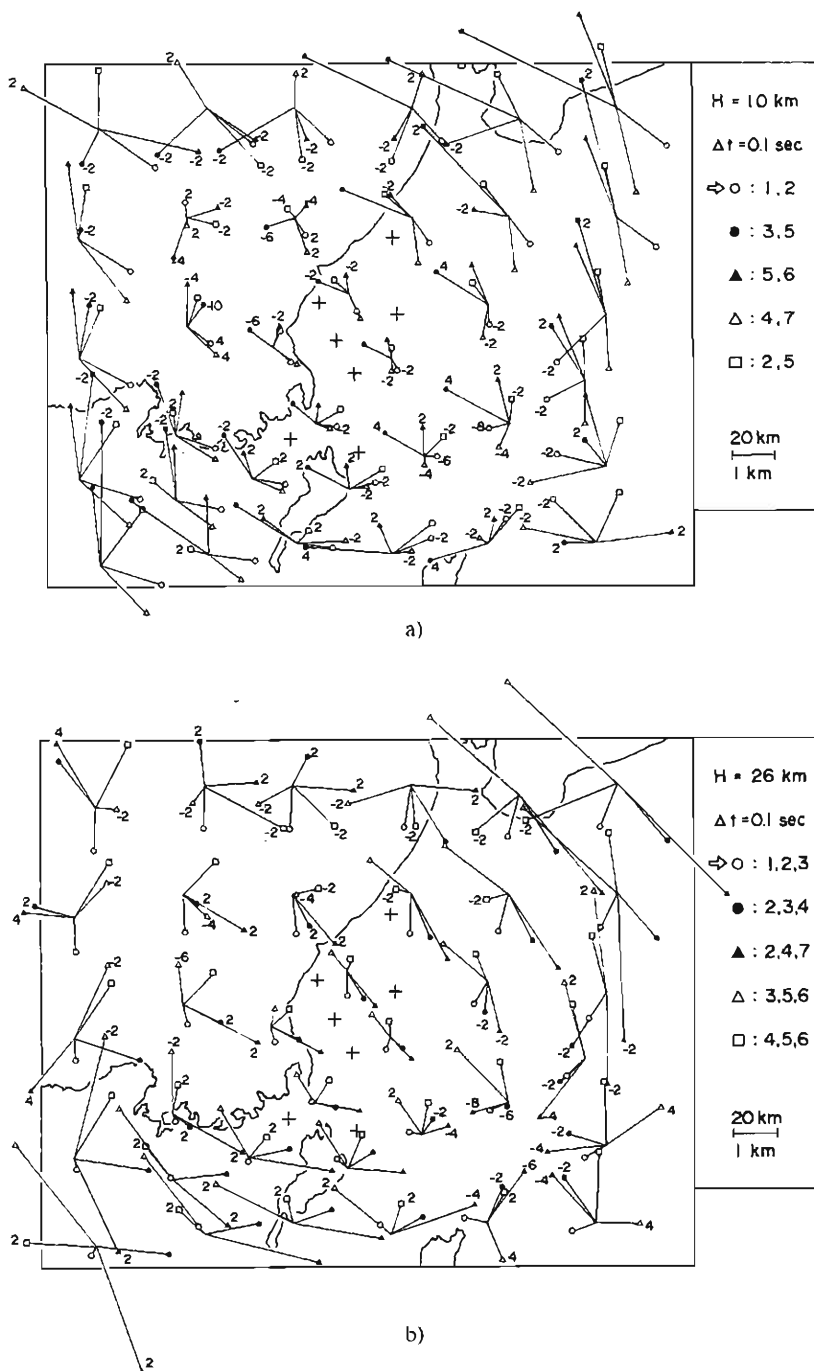


Fig. 9. a) Differences between the fictitious hypocenters and the relocated ones calculated from the data which 0.1 s have been added to each of two P -times. The 5 cases of ${}_{7}C_2$ are shown. Each numeral is the same as in Fig. 7. b) Differences between the fictitious hypocenters and the relocated ones calculated from the data which 0.1 s have been added to each of three P -times. The 5 cases of ${}_{7}C_3$ are shown. Each numeral is the same as in Fig. 7.

and for more than 97% of them, were less than or equal to 2 km except for the events of depths of 38 km. Vertical differences were also less than 2 km for more than 90% of the cases, excluding the case of 38 km in depth. Thus almost all the hypocenters were relocated nearer than 2 km from the initial points. Fig. 8 shows the results of the same kind of examination setting Δt as -0.1 s. The directions of differences concerned with Δt of ± 0.1 s turn to the opposite direction mutually.

4.4.2 Adding Δt to two or three P -times

In this section, we will consider the effects of giving Δt to plural P -times. The number of combinations to pick up n points ($n=1,2,\dots, 7$) out of seven is 127. But here, we exclude the case $n=7$, because it is equivalent to $n=0$. Adding $\Delta t=0.1$ s to four, five and six P -times is equivalent to adding $\Delta t=-0.1$ s to the three, two and one P -times, respectively. And the case $n=1$ has already been tested. So here we have to treat only the case of $n=2$ and 3. Those combinations amount to 56 (${}_{7}C_2+{}_{7}C_3$). The results are listed in Table 3 and 4, and some examples can be seen in Fig. 9. Horizontal differences of about 60% and 90% of the events did not exceed 1 km and 2 km respectively, in both cases of $n=2$ and 3 except for the depth

Table 3. Differences between the fictitious hypocenters and the relocated ones with depths, when the deviation value, Δt , is added to each of two P -times.

Err. dep.	Err.		
	$\Delta \leq 1.0$ km	$\Delta \leq 2.0$ km	$ \text{dep} \leq 2$ km
2 km	60.5%	94.1%	89.1%
6	63.9	94.4	87.2
10	63.8	93.7	91.0
26	62.2	93.6	93.6
38	43.8	71.8	72.2
total = 735			

Table 4. Differences between the fictitious hypocenters and the relocated ones with depth, when the deviation value, Δt , is added to each of three P -times.

Err. dep.	Err.		
	$\Delta \leq 1.0$ km	$\Delta \leq 2.0$ km	$ \text{dep} \leq 2$ km
2 km	58.3%	91.6%	87.4%
6	58.7	91.8	85.9
10	57.1	91.6	89.0
26	55.7	90.7	92.5
38	37.2	66.7	70.8
total = 1225			

of 38 km. Vertical differences were also less than 2 km for 90% of the cases. The differences increase with the number " n ", but the value of differences is not proportional to n . For the effects of adding Δt to some of the P -times cancel each other, and as a result, the difference does not grow so large.

In our routine work, the errors most likely to occur in reading P -times are less than or equal to 0.1 s, as mentioned above. So the hypocenter location errors caused by this analysis method may be about as large as the values listed in Tables 2, 3 and 4.

4.5 Adding Δt to origin times

In this section, we assume that the P -times are read accurately enough and the errors occur only when we read S -phases. To simulate this phenomena, we use the calculated travel times as in the previous sections. In other words, we imagine an earthquake occurring at a time $t=0$, which is the origin time of this initial event, and we catch the seismic waves at our seven stations at the right times. And then we add Δt to the origin time to relocate the hypocenter. The differences between the relocated hypocenters and the initial points are shown in Fig. 10. In the figure, Δt values are taken to be 0.0, ± 0.1 , ± 0.2 and ± 0.5 s. The value 0.5 s is large enough to consider this problem, because the actual reading error rarely exceeds this value as is

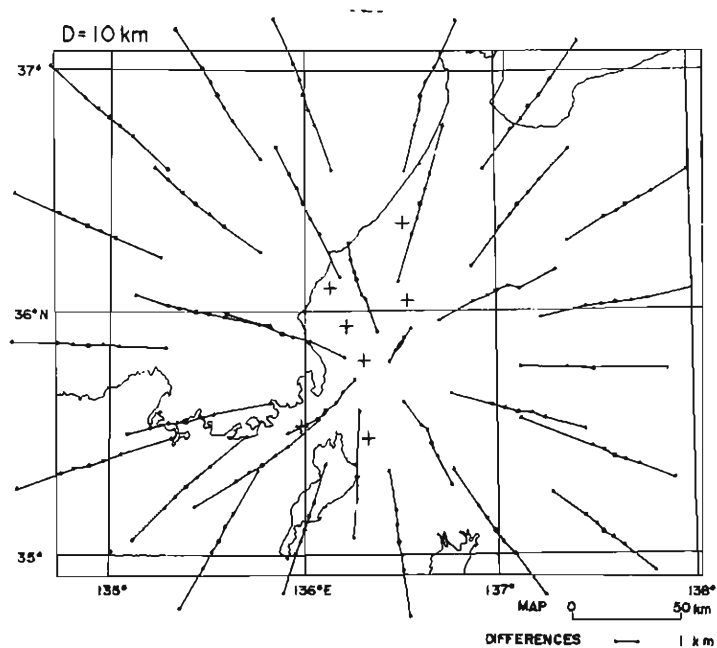


Fig. 10. Differences between the fictitious hypocenters and the relocated ones calculated from the data which the origin times are varied. The larger center point denotes the fictitious one. Other points, forming lines in opposite directions, correspond to the origin time deviation values of ± 0.1 , ± 0.2 and ± 0.5 s respectively.

mentioned above. If Δt equals 0.0 s, the hypocenters are relocated very close to the initial points, which is referred to in section 4.3.

A positive value of Δt shortens the travel times and the epicenter moves nearer to the center of the network. Negative values of Δt work in the opposite sense. The farther the fictitious epicenter is from the network, the larger the difference between the relocated epicenter and the initial one becomes. Near the network, the difference is about 3 km, and about 5 km when outside. Differences of deeper earthquakes are larger than those of shallower ones, if the initial epicenters are the same. The depth of the hypocenter also fluctuates according to Δt . When Δt equals 0, the fluctuation of depths is also 0. But otherwise, the differences may amount to 5 km for the events near the network, but for distant events, the differences are not so large. In short, origin time fluctuation mainly affects the epicenter location of a distant earthquake, and it affects the depth of a nearer event. The averaged rate of the difference to Δt is roughly 3 km/sec.

4.6 The effects of combination of stations

Locations of the seven stations of the Observatory are distributed almost north to south. So we may divide the stations into two groups, one is a group of northern stations, Nos. 1, 2, 3 and 4, and the other is of southern stations, Nos. 4, 5, 6 and 7. We examined the differences between the locations of fictitious hypocenters and the relocated ones of the two groups separately.

Difference values in both cases were almost same as those of the case that all P -times of seven stations were used. But the directions of differences differed much in the two cases (Fig. 11). This may be caused by the relative locations of the event and the

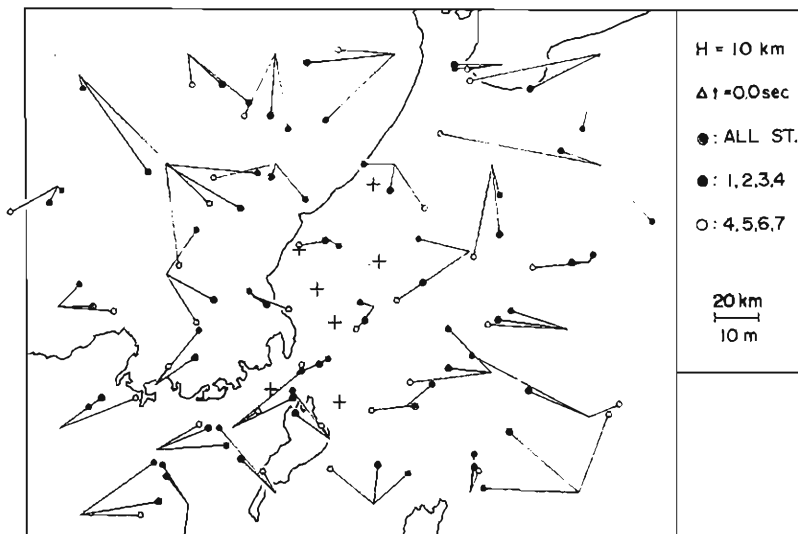


Fig. 11. Hypocenter differences according to the combination of stations.

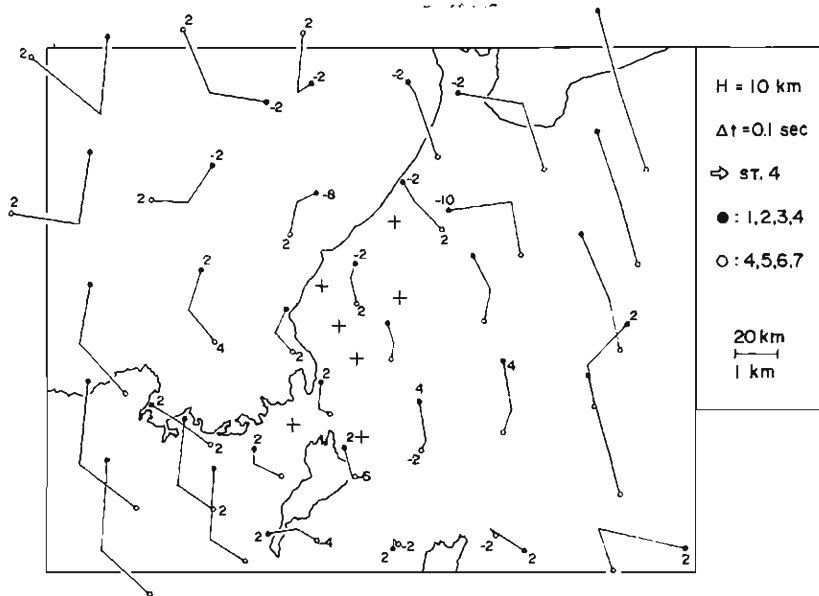


Fig. 12. Effects of the combination of stations when Δt is added to the common station no. 4. Each numeral is the same as in Fig. 7.

stations, and not according to the distances. This characteristic appeared extremely in the case when 0.1 s was given as Δt to P -times of No. 4 station, which belonged to both groups (Fig. 12). The actual data contain more complicated factors of errors, lateral heterogeneity of crustal structure, travel time anomaly peculiar to the station and so on. So these factors should also be taken into account, besides considering the effects of station combinations, to determine hypocenters very accurately.

4.7 The effects of sampling of travel time data

The above arguments were made based on the 11–21 model, which had occupied almost all the core memories of the minicomputer at the Observatory. But recently the computer was graded up and the capacity of memories increased. Then the 27–51 model, a sampled table of travel times at 27 distances from 0 to 300 km for depth of every 1 km from 0 to 50 km, can be memorized at a time and used to determine hypocenters. The differences between the hypocenters relocated by the 27–51 model and the initial positions are outlined in Table 5. In this case, the fictitious travel times were calculated also on the 11–21 model. For shallow events, the differences were large, but for those of depth 38 km, very small.

When the sampling of travel time is rough, the fact that the critical distances of refracted waves from each layer depend on the hypocenters' depths, can not wholly be taken into account. In short, the 11–21 model is not aware that the critical distances of refracted waves from $V_P=7.8$ km/sec layer vary in the range from 100 to 150 km, depending upon the hypocentral depths. This is the cause which explains

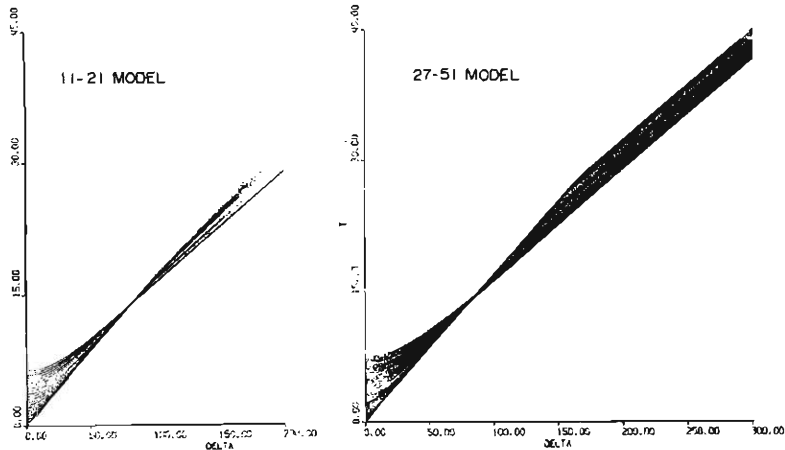


Fig. 13. Travel time curves of 11-21 model and 27-51 model.

Table 5. Hypocenter differences according to the *P*-wave velocity models used in hypocenter determination.

Err. dep.	$\Delta \leq 1.0$ km	$\Delta \leq 2.0$ km	$ \text{dep} \leq 2$ km	$ \text{dep} \leq 6$ km
2 km	57.1 %	74.3 %	20.0 %	42.9 %
6	42.9	65.7	25.7	57.1
10	37.1	65.7	34.3	85.7
26	60.0	74.3	91.4	100.0
38	100.0	—	97.1	100.0
● Mar. 78	77.8	86.7	74.4	90.0

the phenomena above. Fig. 14 shows the differences of the epicenters, which were actually observed by our net stations in March 1978, calculated on the two models. About 80% of the events were located at places near each other on the two models. Large differences occurred with the events distant from the center of the network.

5. Conclusions

The results are as follows:

1) The difference between individual readings of *P*-times was less than 0.1 s for more than 90% of near earthquakes. As for *S*-waves, being converted to origin times, more than 90% of readings were within a difference of 0.5 s.

2) The variations of the relocated epicenters from the fictitious ones were less than 2 km for more than 97% of them, except for the case of 38 km depth. When a probable reading error of *P*-times, 0.1 s, was added to at most three stations, the

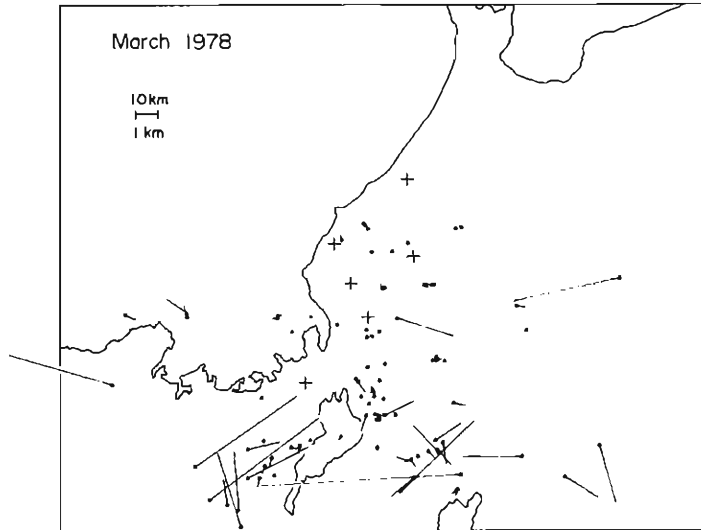


Fig. 14. Differences of the epicenters calculated by the use of the two models. Actually observed data by our network in March 1978 were analyzed.

variations of focal depths were also less than 2 km for more than 90% of them, except for the case of 38 km depth.

3) Adding a probable error of the origin time, 0.5 s, to the origin time mainly affected the depths of hypocenters for near earthquakes and horizontal locations for far ones. When Δt was 0.5 s, the deviations of epicenters were from 3 to 5 km.

4) The effects of combination of the stations to be used can not be disregarded.

5) The strictness of sampling of *P*-wave velocity data also affect the locations of hypocenters to the degree of a few kilometers.

As mentioned above, our analysis method is accurate enough to discuss the seismicity of Hokuriku district, on the condition of the assumed crustal structure. In order to determine more accurate hypocenters, it would be necessary to improve the crustal structure model.

Acknowledgements

The writers wish to express their thanks to Professor Y. Kishimoto and to the other staff members of Microearthquake Research Section of Disaster Prevention Research Institute, Kyoto University for discussions and suggestions on the problem. Numerical computations were run on a FACOM 230/25 at the Information Data Processing Center for Disaster Prevention Research, Disaster Prevention Research Institute, Kyoto University, and on a HITAC 10II at the Hokuriku Microearthquake Observatory.

References

- 1) Tsukuda, T. and S. Nakao: On the Accuracy of Hypocenter Determination by *P* Times at Four Stations of the Tottori Microearthquake Observatory, *Annals, Disast. Prev. Res. Inst., Kyoto University*, No. 20B-1, April, 1978, pp. 47-58.
- 2) Ishii, H. and A. Takagi: On the Detectability of Earthquakes and Crustal Movements in and around the Tohoku District (Northeastern Honshu) (I) Microearthquakes, *Zisin, Ser. 2*, Vol. 31, No. 3, 1978, pp. 287-298.
- 3) Kishimoto, Y., K. Oike, K. Watanabe, T. Tsukuda, N. Hirano and S. Nakao: On the Telemeter Observation System of the Tottori and Hokuriku Micro-earthquake Observatory, *Zisin, Ser. 2*, Vol. 31, No. 3, 1978, pp. 265-274.
- 4) Aoki, H., T. Tada, Y. Sasaki, T. Ooida, I. Muramatsu, H. Shimamura and I. Furuya: Crustal Structure in the Profile across Central Japan as Derived from Explosion Seismic Observations, *J. Phys. Earth*, Vol. 20, 1972, pp. 197-223.
- 5) Mikumo, T., M. Otsuka, T. Utsu, T. Terashima and A. Okada: Crustal Structure in Central Japan as Derived from the Miboro Explosion-Seismic Observations. Part 2. On the Crustal Structure, *Bull. Earthq. Res. Inst., Tokyo University*, Vol. 39, 1961, pp. 327-349.
- 6) Hashizume, M., O. Kawamoto, S. Asano, I. Muramatsu, T. Asada, J. Tamaki and S. Murauchi: Crustal Structure in the Western Part of Japan Derived from the Observation of the First and Second Kurayoshi and Hanabusa Explosions. Part 2. Crustal Structure in the Western Part of Japan, *Bull. Earthq. Res. Inst., Tokyo University*, Vol. 44, 1966, pp. 109-120.